Chemistry for Sustainable Development **8** (2000) 33–38

Principles of the Design of Inorganic Acentric Materials

BORIS I. KIDYAROV[1] and VICTOR I. KOSYAKOV[2]

[1]*Institute of Semiconductor Physics, Siberian Branch of the Russian Academy of Sciences,*
Pr. Akademika Lavrentyeva 13, Novosibirsk 630090 (Russia)

[2]*Institute of Inorganic Chemistry, Siberian Branch of the Russian Academy of Sciences,*
Pr. Akademika Lavrentyeva 3, Novosibirsk 630090 (Russia)

Abstract

The basic principles of chemical design are considered, including the search for new oxide crystals with high piezoelectric properties. A compendium has been composed and the system analysis of a series of physical properties of binary and ternary oxide crystals has been performed on the basis of the key criterion which is the total length of chemical bonds for each component of the oxide compound. A phenomenological model has been proposed to search and classify efficient acentric materials for dielectronics.

INTRODUCTION

Modern materials science and physics of condensed media having investigated many physical properties of the crystals of simple chemical compounds move towards the synthesis, investigation and the analysis of the properties of artificial and natural multicomponent materials and minerals [1–3]. This complex interdisciplinary problem of chemical design includes the tasks connected with the forecast of composition, design of new crystal compounds and various ceramic materials, glass ceramics and glasses, as well as theoretical and phenomenological prediction of their structure and properties [3–8]. Earlier we revealed the empirical model of non-linear optical properties of binary and ternary oxides and matrix methodology of their design that can be also applied to the creation of other acentric and central symmetric crystals, search and forecast of the properties of new solid multicomponent materials possessing the necessary functional properties [2, 3].

In the present paper this model will be discussed in application to the piezoelectric properties of oxides connected with acoustoelectronic and acousto-optical applications of crystals.

THE MODEL OF THE ACENTRIC PROPERTIES OF BINARY OXIDE CRYSTALS

It has been shown in [2, 3] on the basis of the analysis of previous investigations that the most substantial factor that determines the formation of acentric oxide crystals is the length L of the shortest chemical bond metal–oxygen in solid. Its upper limit is 196 pm (L^*) and the lower one is 124.5 pm (L'). For the bond length above $L^* + \delta$ and below $L' - \delta$ all the oxide crystals possess central symmetry while for the bond lengths within $L^* \div L'$ the crystals of both structural types are formed. In the plane of chemical bonds length L(A—O) – L(B—O) the variety of binary acentric oxides $A_nB_mO_p$ is within the rosette composed of two prolonged ellipses and the most efficient among them are exactly in the ellipses line. The set of ternary acentric crystals $A_nB_mC_pO_t$ is located within and on the surface of four ellipsoids formed by rotation and slight deformation of acentric ellipses.

Because of this, the components having bond length shorter than 196 pm will be designated in the chemical formula of multinary oxide as E while those having longer bond length will be designated as L. Then the binary oxide $M^1_nM^2_mO_p$

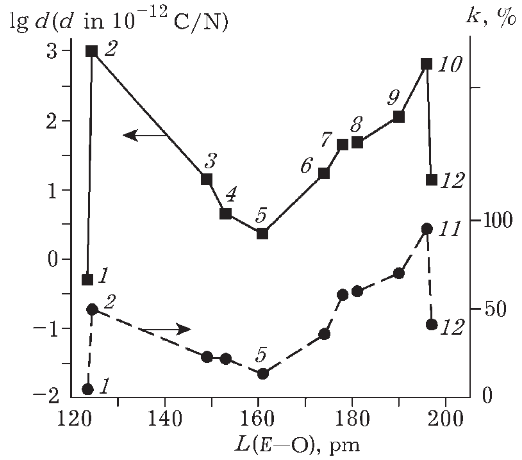

Fig. 1. The dependence of piezomodule d and coefficient of electromechanical coupling k of binary oxides ($M_nE_mO_p$) on the length of the shortest ion-covalent bond L: *1* – $NaNO_2$, *2* – $KNaC_4H_6O_4 \cdot 4H_2O$, *3* –$Cs_2S_2O_6$, *4* –$GaPO_4$, *5* – SiO_2, *6* – Li_2GeO_3, *7* –$KBrO_3$, *8* – α-$LiJO_3$, *9* –$KNbO_3$, *10* – $BaTiO_3$, *11* – $Pb(Zn_{1/3}Nb_{2/3})O_3 \div PbTiO_3$, *12* – ZnO.

possesses central symmetry while $M_nE_mO_p$ and $E^1_nE^2_mO_p$ are acentric or central symmetric. Ternary oxides form four types: $M^1_nM^2_mM^3_pO_t$ – central symmetric and $M^1_nM^2_mE_pO_t$, $M_nE^1_mE^2_pO_t$, $E^1_mE^2_pE^3_nO_p$– acentric or central symmetric. Quaternary oxides form five types: $M^1_nM^2_mM^3_pM^4_tO_v$ are central symmetric, $M^1_nM^2_mM^3_pE_tO_v$, $M^1_nM^2_mE^1_pE^2_tO_v$, $M^1_nE^1_mE^2_pE^3_tO_v$, $E^1_nE^2_mE^3_pE^4_tO_v$ are acentric or central symmetric. Further on, since the shortest bonds govern acentric properties of crystals, within the frames of generalized analysis the classes of simple oxides E_nO_m, binary $E^1_nE^2_mO_p$, $M_nE_mO_p$ and ternary $M^1_nM^1_mE_pO_t$ crystals can be united in one group, together with other multinary crystals possessing at least one bond shorter than 196 pm. Another group of crystals will include those possessing not less than two such bonds. These will be the classes of binary $E^1_nE^2_mO_p$, ternary $M_nE^1_mE^2_pO_t$, and other similar multinary crystals. The third group, respectively, will incorporate the crystals with not less than three such bonds.

The lengths of oxide bonds as a first approximation can be calculated as the sum of efficient crystal ionic octahedral radii or according to the known crystal chemical data [7–9]. The accuracy of mean ionic radii, as well as mean bond lengths, is not better than 5 pm while the lengths of the shortest bonds in specific oxides are determined, by means of X-ray data and other means, with much better accuracy. Within the acentric ellipse, minimal bond length is shorter than the sum of efficient ionic radii of cation and oxygen anion while outside the ellipse it is usually longer. This compression of oxide bond length and inter-oxygen distance is the largest for the smallest cations.

The shortest length of ion-covalent bond $L(E_n$—O) in acentric binary crystal oxides is limited to 107, 123.6 and 196 pm (H_2O, $NaNO_2$, $PbTiO_3$) while the upper limit of the length of the known ionic bond in the oxides of stable elements is ~ 290–310 pm for caesium oxide. Complicated complex compounds exhibit maximum compression of $L(E_n$—O) bond to 0.88 pm. A special case is the occurrence of the hydrogen bond and covalent bond O—H. We estimated the length of hydrogen bond as the half of O—H ··· O distance (124.5 pm) because the proton oscillates statistically in two positions within the mentioned distance.

As in [3], first of all we shall build up the dependence of acentric properties exhibited by the first group oxide crystals (E_nO_m, $E_nE_mO_p$, $M_nE_mO_p$, $M_nM_mE_pO_t$) on the length of the shortest bond L(E—O) (Fig. 1). The data on the maximum components of the piezomodule tensor d in a ranged order, coefficient of electromechanical coupling (CEMC), electrooptical coefficient r, lengths of chemical bonds and classes of structural symmetry for the revealed binary and partly ternary acentric oxides are shown in Table 1. The data are taken from reference books and other literature [3–5, 10–19]. Other tables (which are not shown in this paper) represent the properties of other multinary crystals and are composed similarly. These data are used in further analysis and construction of images.

As one can see from the Table 1, the list of efficient acentric oxide crystals is not too large at present. These crystals belong to polar classes of symmetry (ferroelectrics) and to a limited number of the classes of chemical compounds. In spite of incomplete in-phase coincidence between d, r and CEMC, all these values

TABLE 1

Piezoelectric (d, CEMC) and electrooptical (r) properties of binary and ternary oxide crystals

Formula	Structure	L(B—O), pm		CEMC, %	r, pm/V	d, 10^{-12} C/N
		A—O	B—O			
$KNaC_4H_4O_6 \cdot 4H_2O$	C_2	127	124.5	50	17.7	383-2333
$BaTiO_3$	C_{4v}	275	196	75.2	1640	587
$PbTiO_3$	C_{4v}	259	196	78	13.8	117−193
$KNbO_3$	C_{2v}	278	190		450	107
$LiNbO_3$	C_{3v}	206	190	68	32.2	78
$Li_{0.7}H_{0.3}JO_3$	C_6	124.5	180			67
$NH_4H_2PO_4$	D_{2d}	289	140	30	24.5	52.3
$Ba_2NaNb_5O_{15}$	C_{2v}	275	190	57	92	52
α-$LiJO_3$	C_6	204	180	60	9.8(6.4)	46.3
$KBrO_3$	D_3	278	178	58	10	40
$Ca_2Nb_2O_7$	C_2	240	190		25.5	40
$Bi_{12}SiO_{20}$	T	240	161	31	3.3	40
KJO_3	C_2	278	182		~3	39
α-HJO_3	D_2	124.5	180		8.8	32.5
$LiTaO_3$	C_{3v}	206	190	41	30.3(44)	26
$K_2C_4H_4O_6 \cdot H_2O$	C_2	278	127			23
KH_2PO_4	D_{2d}	278	140	22	10.5	20.9
$3La(JO_3)_3 \cdot HJO_3 \cdot 7H_20$	D_{2d}	124.5	180			19
Li_2GeO_3	C_{2v}	206	174	36		17
$LiCOOH \cdot H_2O$	C_{2v}	206	127	17.2		15.6
$Cs_2S_2O_6$	C_{6v}	307	150		6.17	14.7
ZnO	C_{6v}	197	197	41	2.6	13.9
$Sr(COOH)_2$	D_2	258	157		3.16	11.5
$LiGaO_2$	C_{2v}	206	195	30		8.6
$Li_2SO_4 \cdot H_2O$	C_2	206	151		8.5	7.1
$Pb_5Ge_3O_{11}$	C_3	259	174		16	6.2
$LiClO_4 \cdot 3H_2O$	C_{6v}	206	144	8.3	6.61	5.37
$Ba(COOH)_2$	D_2	275	127		2.03	5.15
$Sr(COOH)_2 \cdot H_2O$	D_2	127	140		2.03	5.13
$Gd_2(MoO_4)_3$	C_{2v}	234	183	3.0	4.1	4
$Ba(NO_2)_2 \cdot H_2O$	C_6	275	123.6	3.4	3.47	3.1
$NaClO_3$	T	242	157		0.4	2.7
α-TeO_2	D_4	188	188	10		2.44
$AlPO_4$	D_3	193	154	22		
$GaPO_4$	D_3	201	154	22		4.5
α-SiO_2	D_3	161	161	13.7	0.47	2.3
$Bi_4(GeO_4)_3$	T_{d}	242	174	1.5	1.03	0.87
$Ba_2Si_2TiO_8$	C_{4v}	161	196	34	5.9	18
$RbHC_8H_4O_4$	D_2	124.5	127	33.9	0.03	12
$KHC_8H_4O_4$	D_2	124.5	127	24.4		8.8
Na_2CoGeO_4	D_2	240	174	25.5		9.4

exhibit increasing at the beginning of the table. Further analysis allows to establish a more detailed correlation of data from Table 1. Figure 1 shows the projection of all the largest components of piezomodule tensor $d(M_nE_mO_p)$ and the coefficient of electromechanical coupling k of oxide crystals to the plane $d - L(E$—O). The envelope of the largest components of the tensor $d_{\max}(M_nE_mO_p) = f\ \{L(\mathrm{E—O})\}$ is truncated because the argument region (in which the function is defined) is limited by the above-mentioned bond length limit. For the

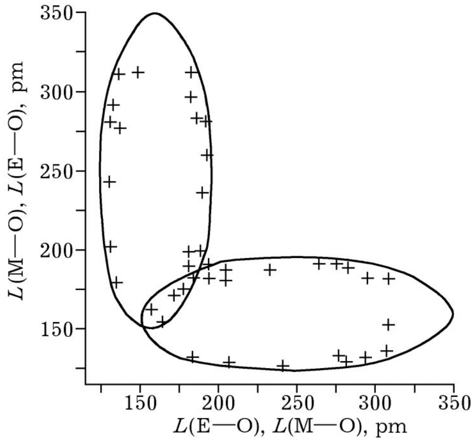

Fig. 2. The coordinates of the most efficient binary acentric crystals $M_nE_mO_p$ on the plane of chemical bond lengths L(M—O) – L(E—O).

bonds shorter than 107 pm, no oxide compounds exist. Within the region of bond lengths longer than 196 pm there are antiferroelectric and central symmetrical oxide phases for which (d, k) are zero. For all the other acentric binary oxides, $d_{\max}(M_nE_mO_p)$ are located below this shape so that the lower envelope, which is zero for central symmetrical phases, coincides with the abscissa axis.

In spite of large scattering of all the acentric properties, their upper envelope for each curve in this plot is clearly seen to form two out-of-phase branches. They cross each other in the minimum which is located in the centre of the ellipse L(E—O) = 160 pm (this is approximately silicates, selenites). The left branch of the dependence is formed by the oxides possessing either hydrogen or oxygen π–bond (nitrites, nitrates, hydroxides, crystal hydrates, formiates, carbonates, acetates, oxalates, tartrates, borates, sulphites, perchlorates, sulphates, phosphates, chlorates, silicates). The right branch is formed by the oxides with σ-bond (selenates, chromates, germanates, arsenates, selenites, bromates, periodates, iodates, molybdates, tungstates, vanadates, niobates, aluminates, titanates, zincates, gallates, manganates). The maximum of acentric properties of oxides is located at bond length equal to hydrogen bond (ferroelectrics of the "order-disorder" type) and titanate bond (ferroelectrics that undergo phase transformations of the displacement type). So, the maximum of acentric properties of binary oxides is observed in the least stable lattices that usually change crystal structure as a result of the variations in chemical composition or state parameters.

At the next stage we are to build up an empirical dependence of the largest components (among those symmetrically allowed) of the piezoelectric module (or the coefficient of electromechanical coupling) of binary oxides on two arguments, namely, on the shortest lengths of chemical bonds, ionic bond (M—O) and ion-covalent bond (E—O). The total projection of the coordinates of the most efficient piezoelectric binary oxides ($d(M_nE_mO_p) = f\ \{L(\text{M—O}), L(\text{E—O})\}$) in the plane of the lengths of these bonds is shown in Fig. 2. It is clearly seen that the mentioned line of maximum values is an ellipse prolonged over the M—O-axis. Transposition of arguments order in the function leads to the rotation of the ellipse around the axis of equal distances (the axis of simple oxides) and exchange of the minor axis in the ellipse for the focal one and *vice versa*. So, we obtain a rosette composed of two ellipses with focal axes that cross each other in the lower focus of ellipse; the axis of equal distances is the symmetry axis of this rosette. The equation of the ellipse is identical to that obtained earlier for the analysis of non-linear optical properties of crystals [3] and is quite the same when composed for all the other acentric properties of the crystals.

In each section of the ellipse passing through its centre the function under consideration is to a first approximation a truncated shape similar to those shown in Fig. 1, with the minimum close to zero at the centre of ellipse and two maxima at its edges. The parameters of the ellipses of acentricity, as well as the tolerance factor, are generalized criteria that characterize the ability of oxide compound to form acentric lattice. They are determined for the minor axis by the relation of cation radii to the size of tetrahedral and octahedral hollows in the tight oxygen sublattice of oxides while on the focal axis the coordinate of the ellipse centre is equal to the shortest distance between oxygen ions [3].

On the minor axis of the ellipse, the maximum of acentric properties is observed for close coincidence between the size of the

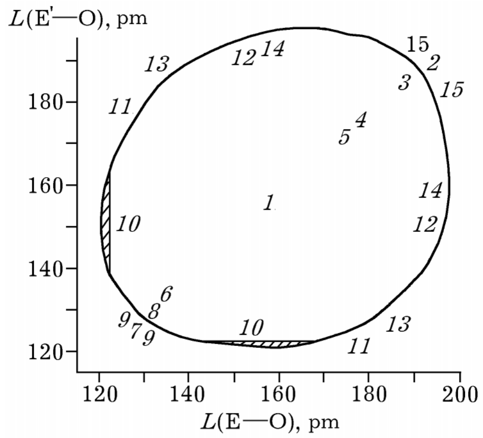

Fig. 3. The total projection of the coordinates of the most efficient ternary acentric crystals of the type $M_nE^1_mE^2_pO_t$ on the plane of chemical bonds lengths $L(E^1—O) - L(E^2—O)$: *1* – SiO_2, *2* – $BaTiO_3$, $PbTiO_3$, *3* – $KNbO_3$, *4* – KJO_3, $LiJO_3$, *5* – $KBrO_3$, *6* – BaB_2O_4, *7* – KNO_3, *8* – $(NH_4)_2C_2O_4 \cdot 1/2H_2O$, *9* – $KNaC_4H_6O_4 4H_2O$, *10* – KH_2PO_4, *11* – HJO_3, *12* – $KTiOPO_4$, *13* – KB_2NbO_6, *14* – $BaSiTiO_8$, *15* – $Ba_6Ti_2Nb_8O_{30}$.

minorest cation with the size of octahedral or tetrahedral hollow of the sublattice composed of the ions of oxygen, chalcogen or another element (in oxides, chalcogenides or pnictides, respectively). On the basis of the above, this circumstance allows to predict, as a first approximation, a similar ellipse equation for other simple and binary inorganic compounds. Really, having determined the coordinates of the edge points of the ellipse as described above, we can determine the coordinate of the ellipse centre on the minor axis as the half-sum of these values; on the focal axis these coordinates are approximately equal to the interanion distance. The coordinates of the focus points in the ellipse are determined as the cross point of the focal axis and the line of equal distances.

THE SCHEME OF THE ANALYSIS OF ACENTRIC PROPERTIES OF TERNARY OXIDES

For ternary oxides, piezoelectric properties are a function of three arguments ($d(M_nE_mE_pO_t) = f$ {L(M—O), L(E—O), L(E—O)} or $d(M_nM_m E_pO_t) = f$ {L(M—O), L(M—O), L(E—O)}). Earlier we considered non-linear optical properties of barium and potassium compounds, the best studied class of these oxides [3]. In the present work we show in Fig. 3 in the plane of ion-covalent bond lengths $L(E^1—O) - L(E^2—O)$ the general projection of the lengths of oxide bonds of all the acentric crystals of the type ($M_nE^1_mE^2_pO_t$) and binary ones of the type $E^1_mE^2_pO_t$ taken from Table 1 and ref. [3, 10–19]. Here we marked the line in which the most efficient piezoelectric crystals are located. For these compounds, the maximum $d(M_nE^1_mE^2_pO_t) = f$ {$L(E^1—O)$, $L(E^2—O)$} is observed for the compounds HJO_3, KJO_3, $LiJO_3$, $KBrO_3$, $KNbO_3$, BaB_2O_4, KH_2PO_4, $KBNb_2O_6$, $Ba_6Ti_2Nb_3O_{30}$, $Ba_2Si_2TiO_8$, $BaTiO_3$, $PbTiO_3$, $KTiOPO_4$ while other crystals are characterized by lower acentric properties. One can see that the mentioned line is an ellipse practically equal to the ellipse obtained earlier for ternary compounds with barium and potassium oxides. These ellipses are also slightly prolonged along the axis of equal chemical bond lengths [3]. In the marked left and lower part of the ellipse no acentric ternary oxides have been discovered yet, since the minimum of hydrogen bond and N—O chemical bond is longer than 123.6 pm. Because of this, these two imaginary segments of the ellipse are shadowed (see Fig. 3). The mentioned lower left part of the ellipse is built as the reflection of its upper right part.

The model under consideration allows to analyse similarly the properties of other polycomponent crystals by considering binary and ternary cross sections of the corresponding geometric image in a multidimensional space.

This analysis is correct only for oxides with the composition close to stoichiometric ratio of the comprising components and approximately equal to 1 : 1 or 1 : 1: 1 for ternary oxides. For other types of composition of multicomponent oxides, it is necessary to introduce a correction for the acidity (basicity) of oxide mixtures, or to make additional constructions of special type which will be considered in further works.

It is known that the fraction of acentric crystals is about 30 % of their total number. The area of the ellipses of acentricity occupies about 60 % of the plot of the chemical bond lengths of binary oxides. It contains also quite the same fraction of the crystals possessing central symmetric structure and practically all the acentric crystals. This means that within the ellipse of acentricity the fraction of acentric crystals will be about 50 %. Limiting the regions where we search for acentric oxide crystals to the area of the ellipse "belt" adjacent from inside to the ellipse of acentricity and taking ~ 50 % of its area, we exclude ~ 70 % of less promising crystal search regions, thus increasing the efficiency of preliminary forecast more than three times.

CONCLUSION

Thus, the features of chemical bond and crystallochemical principles of the composition of oxide crystals govern also the model of their general physical properties. The revealed ellipse of acentricity is observed and exhibits itself during the analysis of different physical properties of both acentric and central symmetric inorganic crystals. The possibility to construct such an ellipse *a priori* much helps the forecasting analysis of functional properties and the search for new materials. A minimal length of chemical bond is connected with the short-range order in condensed media. So, definite regularities similar to those mentioned above should be observed also for noncrystalline media. Taking into account the above statements, it is very urgent that we should consider the minimal length of chemical bonds along with lattice parameters and other values when studying and composing databases on the structural characteristics of substances. At present, theoretical prediction of the structure and properties of crystals is yet impossible, in spite of the success achieved. The solution of these problems requires further development and comparisons between different approaches to the analysis of the properties of multicomponent materials. Because of this, the phenomenological model described herein is useful both for the development of theory and for methodology of classification, search and synthesis of new promising materials.

REFERENCES

1 N. N. Kiselyova, *Zhurn. neorgan. khimii*, 42 (1997) 896.

2 B. I. Kidyarov and V. I. Kosyakov, Proc. of SPIE, vol. 3485, 1998, p. 385.

3 B. I. Kidyarov and E. V. Pestryakov, *Izv. RAN. Ser fiz.*, 63 (1999) 1080.

4 I. S. Rez and Yu. M. Poplavko, Dielektriki. Osnovnye svoystva i primeneniye v elektronike, Radio i svyaz', Moscow, 1989.

5 S. C. Abrahams, *Acta Cryst.*, B46 (1990) 311.

6 B. V. Beznosikov and K. S. Aleksandrov, Trudy II Mezhdunar. konf. "Real'naya struktura i svoystva atsentrichnykh kristallov",VNIISIMS, Aleksandrov, 1995, p. 79.

7 V. S. Urusov, Teoreticheskaya kristallokhimiya, Izd-vo MGU, Moscow, 1987.

8 I. Narai-Szabo, Neorganicheskaya kristllokhimiya, Akademiai Kiado, Budapest, 1969.

9 R. D. Shannon and C. T. Prewitt, *Acta Cryst.*, 25 B, 20 (1969) 1046.

10 A. M. Prokhorov (Ed.), Spravochnik po lazeram, vol. 2, Sov. Radio, Moscow, 1978.

11 A. A. Blistanov, V. S. Bondarenko, V. V. Chkalova *et al.*, in M. P. Shaskol'skaya (Ed.), Akusticheskiye kristally: Spravochnik, Nauka, Moscow, 1982.

12 S. Haussuhl, J. Liebertz, *Zeitschrift für Krystallographie*, 148 (1978) 87.

13 S. Haussuhl, *J. Appl. Cryst.*, A 34 (1978) 547.

14 S. Haussuhl, *Phys. Stat. Sol.,* 6a (1971) K23.

15 S. Haussuhl, *Acta Cryst.,* 33a (1977) 320.

16 M. P. Zaytseva, L. A. Shabanova, B. I. Kidyarov *et al.*, *Kristallografiya*, 28 (1983) 741.

17 R. Liminga, S. C. Abrahams and J. L. Bernstein, *J. Appl. Cryst.*, 13 (1980) 516.

18 G. A. Smolensky, V. A. Bokov, V. A. Isupov *et al.*, Segnetoelektriki i antisegnetoelektriki, Nauka, Leningrad, 1973.

19 M. S. Madhava, S. Haussuhl, *Zeitschrift für Kristallographie,* 142 (1975) 322.